

Performance of Orthogonal Beamforming for SDMA with Limited Feedback

Kaibin Huang, Jeffrey G. Andrews, and Robert W. Heath, Jr

Abstract

On the multi-antenna broadcast channel, the spatial degrees of freedom support simultaneous transmission to multiple users. The optimal multiuser transmission, known as dirty paper coding, is not directly realizable. Moreover, close-to-optimal solutions such as Tomlinson-Harashima precoding are sensitive to CSI inaccuracy. This paper considers a more practical design called per user unitary and rate control (PU2RC), which has been proposed for emerging cellular standards. PU2RC supports multiuser simultaneous transmission, enables limited feedback, and is capable of exploiting multiuser diversity. Its key feature is an orthogonal beamforming (or precoding) constraint, where each user selects a beamformer (or precoder) from a codebook of multiple orthonormal bases. In this paper, the asymptotic throughput scaling laws for PU2RC with a large user pool are derived for different regimes of the signal-to-noise ratio (SNR). In the multiuser-interference-limited regime, the throughput of PU2RC is shown to scale logarithmically with the number of users. In the normal SNR and noise-limited regimes, the throughput is found to scale double logarithmically with the number of users and also linearly with the number of antennas at the base station. In addition, numerical results show that PU2RC achieves higher throughput and is more robust against CSI quantization errors than the popular alternative of zero-forcing beamforming if the number of users is sufficiently large.

I. INTRODUCTION

In multi-antenna broadcast channels, simultaneous transmission to multiple users, known as multiuser multiple-input-multiple-output (MIMO) or *space division multiple access* (SDMA), is capable of achieving much higher throughput than other multiple-access schemes such as *time division multiple access* (TDMA) [1]. Due to this advantage, SDMA has been recently included in the IEEE 802.16e standard [2], and has been proposed for the emerging 3GPP long term evolution (LTE) standard [3]–[6]. While the optimal SDMA strategy is known, *dirty paper coding* [7] is non-causal and hence not directly realizable. Moreover, close-to-optimal techniques such as Tomlinson-Harashima precoding and vector perturbation are sensitive to CSI

The authors are with Wireless Networking and Communications Group, Department of Electrical and Computer Engineering, The University of Texas at Austin, 1 University Station C0803, Austin, TX 78712. Email: huangkb@mail.utexas.edu, {jandrews, rheath}@ece.utexas.edu. Kaibin Huang is the recipient of the University Continuing Fellowship from The University of Texas at Austin. This work is funded by the DARPA IT-MANET program under the grant W911NF-07-1-0028, and the National Science Foundation under grants CCF-514194 and CNS-435307. The results in this paper were presented in part at the IEEE Int. Conf. Acoust., Speech and Sig. Proc., Apr. 2007.

inaccuracy [8], [9]. More practical SDMA algorithms are based on transmit beamforming, including zero forcing [10]–[13], a signal-to-interference-plus-noise-ratio (SINR) constraint [14], minimum mean squared error (MMSE) [15], and channel decomposition [16]. These SDMA algorithms can be combined with multiuser scheduling to further increase the throughput by exploiting *multiuser diversity*, which refers to scheduling only a subset of users with good channels for each transmission [17]–[23]. Both scheduling and beamforming in a SDMA system require channel state information (CSI) at the base station. Unfortunately, CSI feedback from each user potentially incurs excessive overhead because of the multiplicity of channel coefficients. Therefore, this paper focuses on SDMA that supports efficient CSI feedback and uses CSI for joint beamforming and scheduling.

A. Related Work and Motivation

In this paper, we consider a practical scenario where partial CSI is acquired by the base station through quantized CSI feedback, known as *limited feedback* [24]. Quantized CSI feedback for point-to-point communications has been extensively studied recently (see e.g. [24], [25] and the references therein). The effects of CSI quantization on a SDMA system have been investigated in [20], [26], [27]. The key result of [20] is that the number of CSI feedback bits can be reduced by exploiting multiuser diversity. In [26], combined quantized CSI feedback and zero-forcing dirty paper coding are shown to attain most of the capacity achieved by perfect CSI feedback. In [27], it is shown that for a small number of users the number of CSI feedback bits must increase with the signal-to-noise ratio (SNR) to ensure that the throughput grows with SNR.

This paper addresses joint beamforming and scheduling for SDMA systems to maximize throughput, assuming backlogged users. A similar scenario but with bursty data and the objective of meeting quality-of-service (QoS) for different users is addressed in [28] and references therein. The optimal approach for our full-queue scenario involves an exhaustive search, where for each possible subset of users a corresponding set of beamforming vectors is designed using algorithms such as that proposed in [14]. The main drawback of the optimal approach is its complexity, which increases exponentially with the number of users. This motivates the designs of more efficient SDMA algorithms.

In [22], a practical SDMA algorithm, called *opportunistic SDMA* (OSDMA), is proposed, which supports low-rate beamforming feedback and satisfies the orthogonal beamforming constraint. As shown in [22], for a large number of users, an arbitrary set of orthogonal beamforming vectors ensures that the throughput increases with the number of users at the optimal rate. Nevertheless, for a small number of users, such arbitrary beamforming vectors are highly sub-optimal due to excessive interference between scheduled users. To reduce multiuser interference caused by sub-optimal beamforming vectors, an extension of OSDMA, called *OSDMA with beam selection* (OSDMA-S), is proposed in [21], where each mobile iteratively selects

beamforming vectors broadcast by the base station and sends back its choices. Due to distributed beam selection, numerous iterations of broadcast and feedback are required for implementing OSDMA-S, which incurs significant downlink overhead and feedback delay. As a result, the throughput gains of OSDMA-S over OSDMA are marginal.

An alternative beamforming SDMA algorithm is proposed in [20], referred to as ZF-SDMA, where feedback CSI is quantized using the *random vector quantization* (RVQ) algorithm [27], [29] and greedy-search scheduling is performed prior to zero-forcing beamforming. A design similar to ZF-SDMA [6] has been proposed to the emerging 3GPP-LTE standard [3], which is the latest cellular communication standard. The drawback of ZF-SDMA is its lack of robustness against CSI inaccuracy due to the separate designs of the limited feedback, scheduling and beamforming sub-algorithms.

In industry, SDMA with orthogonal beamforming, under the name *per user unitary and rate control* (PU2RC) [5], has been proposed to the 3GPP-LTE standard. The main feature of PU2RC is limited feedback, where multiuser precoders or beamformers are selected from a codebook of multiple orthonormal bases. Based on limited feedback, PU2RC supports SDMA, scheduling, and adaptive modulation and coding. Because of its versatility and advanced features, PU2RC is one of the most promising solutions for high-speed downlink in 3GPP-LTE. The importance of PU2RC for the next-generation wireless communication motivates the investigation of its performance in this paper.

In this paper, we consider a simplified PU2RC system where scheduled users have single data streams, which are separated by orthogonal beamformers. In this case, PU2RC generalizes OSDMA [22] by allowing the beamforming codebook to contain more than one orthonormal basis. Such a generalization complicates the performance analysis of PU2RC because the resultant scheduler is more complicated. To be specific, the scheduler has to select an orthonormal basis from the codebook besides choosing a particular user for each codebook vector. Such a challenge motivates our use of a new analytical tool, namely *uniform convergence in the weak law of large numbers* [30], for analyzing the throughput of PU2RC instead of *extreme value theory* as applied in [22].

Theory of uniform convergence in the weak law of large numbers is also applied in our previous work [31] for analyzing the throughput of uplink SDMA with limited feedback. Despite using the same tool, the analysis in this paper differs from [31] due to differences between the uplink and downlink. Specifically, the received data signal for the downlink propagates through a single-user channel, but that for the uplink passes through multiuser channels. As a result, SINR feedback for downlink SDMA is infeasible for uplink SDMA, where SINR depends on multiuser CSI and is hence uncomputable at users. Consequently, downlink and uplink SDMA require different designs of scheduling algorithm. Thus, the joint beamforming and scheduling algorithm presented in this paper is not applicable for uplink SDMA. Interestingly, despite the differences

between the uplink and downlink, the asymptotic throughput scaling laws for downlink SDMA as derived in this paper are found to be identical to those for uplink SDMA [31].

B. Contributions and Organization

The main contribution of this paper is the analysis of the throughput scaling of PU2RC for an asymptotically large number of users $U \rightarrow \infty$. Using the theory of uniform convergence in the weak law of large numbers, throughput scaling laws are derived for three regimes, namely the *normal SNR*, *interference-limited* and the *noise-limited* regimes. In the normal SNR regime, both the variance of noise and multiuser interference are comparable; in the interference-limited regime, multiuser interference dominates over noise; the reverse exists in the noise-limited regime. Our main results are summarized as follows. In the interference-limited regime, we show that the throughput scales *logarithmically* with U but does not increase with the number of transmit antennas N_t at the base station. In both the normal SNR and noise-limited regimes, we show that the throughput scales *double logarithmically* with U and *linearly* with N_t . This throughput scaling law shows that PU2RC achieves the optimal multiuser diversity gain as OSDMA in the normal SNR regime¹. Thereby, this result contradicts the intuition that using multiple orthonormal bases in the codebook splits the user pool and hence reduces the multiuser diversity gain. Using Monte Carlo simulations, the asymptotic throughput scaling laws are also found to hold in the non-asymptotic regime where U is finite.

The asymptotic throughput analysis for PU2RC provides several guidelines for designing the scheduler to ensure optimal throughput scaling. First, in the interference-limited regime, scheduling should use the criterion of minimum quantization error. Second, in the normal SNR regime, scheduled users should have both large channel power and small quantization errors. Third, in the noise-limited feedback, scheduling should select users with large channel power while the quantization error is a less important scheduling criterion.

Numerical results are presented for evaluating the throughput of PU2RC and also comparing PU2RC with ZF-SDMA. Several observations are made. First, increasing the amount of CSI feedback (or the codebook size) can decrease the throughput for PU2RC if the number of users is small. Otherwise, more CSI feedback provides a throughput gain. Second, PU2RC achieves higher throughput than ZF-SDMA for large numbers of users but the reverse holds for relatively small numbers of users. Third, decreasing the codebook size causes a larger throughput loss for ZF-SDMA than that for PU2RC.

The remainder of this paper is organized as follows. The system model is described in Section II. The sub-algorithms of PU2RC for CSI quantization, and joint beamforming and scheduling are presented in Section III. The asymptotic throughput scaling of PU2RC is analyzed in Section IV. The performance

¹The interference-limited and noise-limited regimes have not been considered for OSDMA in [22]

of PU2RC is evaluated using Monte Carlo simulation in Section V, followed by concluding remarks in Section VI.

II. SYSTEM MODEL

The downlink or broadcast system illustrated in Fig. 1 is described as follows. The base station with N_t antennas transmits data simultaneously to N_t active users chosen from a total of U users, each with one receive antenna. The base station separates the multiuser data streams by beamforming, i.e. assigning a beamforming vector to each of the N_t active users. The beamforming vectors $\{\mathbf{w}_n\}_{n=1}^{N_t}$ are selected from multiple sets of unitary orthogonal vectors following the beam and user selection algorithm described in Section III-B. Equal power allocation over scheduled users is considered². The received signal of the u th scheduled user is expressed as

$$y_u = \sqrt{\frac{P}{N_t}} \mathbf{h}_u^\dagger \sum_{n \in \mathcal{A}} \mathbf{w}_n x_n + \nu_u, \quad u \in \mathcal{A}, \quad (1)$$

where we use the following notation

N_t	number of transmit antennas and also number of scheduled users;	\mathbf{w}_u	$(N_t \times 1$ vector) beamforming vector with $\ \mathbf{w}_u\ ^2 = 1$;
\mathbf{h}_u	$(N_t \times 1$ vector) downlink channel;	\mathcal{A}	The index set of scheduled users;
x_u	transmitted symbol with $E[x_u ^2] = 1$;	P	transmission power; and
y_u	received symbol;	ν_u	AWGN sample with $\nu_u \sim \mathcal{CN}(0, 1)$.
\dagger	conjugate transpose matrix operation;		

For the purpose of asymptotic analysis of PU2RC, we make the following assumption:

Assumption 1: The downlink channel $\mathbf{h}_u \forall u = 1, 2, \dots, U$ is an i.i.d. vector with $\mathcal{CN}(0, 1)$ coefficients.

Given this assumption commonly made in the literature of SDMA and multiuser diversity [18], [19], [21], [22], [27], the channel direction vector $\mathbf{h}_u / \|\mathbf{h}_u\|$ of each user follows a uniform distribution. Assumption 1 greatly simplifies the throughput analysis of PU2RC in Section IV but has no effect on the PU2RC algorithms in Section III. Assumption 1 is valid for the scenario where wireless channels have rich scattering and users encounter equal path loss. Throughput analysis for a more complicated channel model is a topic for future investigation.

III. ALGORITHMS

In this section, we propose the algorithms for PU2RC including (i) limited feedback by the mobiles and (ii) joint beamforming and scheduling at the base station. The principles for these algorithms have been

²Note that equal power allocation is close to the optimal water-filling method if scheduled users all have high SINR.

described in the proposal of PU2RC [5] even though their details are not provided therein. The algorithms presented in the following sections are tailored for the system model in Section II. The following discussion on algorithms serves two purposes: (i) to elaborate the operation of PU2RC and (ii) to establish an analytical model for the asymptotic throughput analysis in Section IV.

A. Limited Feedback

Without loss of generality, the discussion in this section focuses on the u th user and the same algorithm for CSI quantization is used by other users. For simplicity, we make the following assumption

Assumption 2: The u th user has perfect CSI \mathbf{h}_u .

This assumption allows us to neglect the channel estimation error at the u th mobile. For convenience, the CSI, \mathbf{h}_u , is decomposed into two components: the *gain* and the *shape*. Hence,

$$\mathbf{h}_u = g_u \mathbf{s}_u, \quad u = 1, \dots, U, \quad (2)$$

where $g_u = \|\mathbf{h}_u\|$ is the gain and $\mathbf{s}_u = \mathbf{h}_u / \|\mathbf{h}_u\|$ is the shape. The u th user quantizes and sends back to the base station two quantities: the *channel shape* and the SINR.

The channel shape \mathbf{s}_u is quantized using a codebook-based quantizer [32] with a codebook comprised of multiple sets of orthonormal vectors in \mathbb{C}^{N_t} . Let \mathcal{F} denote the codebook, $\mathcal{V}^{(m)}$ the m th orthonormal set in the codebook, and M the number of such sets. Thus, $\mathcal{F} = \bigcup_{m=1}^M \mathcal{V}^{(m)}$ and the codebook size is $N = |\mathcal{F}| = MN_t$. For our design, the M orthonormal bases of \mathcal{F} are generated randomly and independently using a method such as that in [33]. Following [34] and [35], the quantized channel shape, represented by $\hat{\mathbf{s}}_u$, is the member of \mathcal{F} that forms the smallest angle with the channel shape \mathbf{s}_u . Mathematically,

$$\hat{\mathbf{s}}_u = \arg \min_{\mathbf{v} \in \mathcal{F}} d(\mathbf{v}, \mathbf{s}_u), \quad (3)$$

where the distortion function $d(\mathbf{v}, \mathbf{s}_u)$ is given as

$$d(\mathbf{v}, \mathbf{s}_u) = 1 - \left| \mathbf{v}^\dagger \mathbf{s}_u \right|^2 = \sin^2(\angle(\mathbf{v}, \mathbf{s}_u)). \quad (4)$$

It follows that the *quantization error* can be defined as $\epsilon = \sin^2(\angle(\hat{\mathbf{s}}_u, \mathbf{s}_u))$. It is clear that $\epsilon = 0$ if $|\hat{\mathbf{s}}_u^\dagger \mathbf{s}_u| = 1$ and $\epsilon = 1$ if $\hat{\mathbf{s}}_u \perp \mathbf{s}_u$.

The quantized channel shape $\hat{\mathbf{s}}_u$ is sent back to the base station through a finite-rate feedback channel [24], [34]. Since the quantization codebook \mathcal{F} can be known *a priori* to both the base station and mobiles, only the index of $\hat{\mathbf{s}}_u$ needs to be sent back. Therefore, the number of feedback bits per user for quantized channel shape feedback is $\log_2 N$ since $|\mathcal{F}| = N$. The number of additional bits required for SINR feedback is discussed in Section V.

Besides the channel shape, the u th user also sends back to the base station the SINR, which serves as a channel quality indicator. For orthogonal beamforming, the SINR is given as [20]

$$\text{SINR}_u = \frac{\gamma \rho_u (1 - \epsilon_u)}{1 + \gamma \rho_u \epsilon_u}, \quad (5)$$

where $\gamma = \frac{P}{N_t}$ is the SNR, ϵ_u the CSI quantization error, and $\rho_u = \|\mathbf{h}_u\|^2$ the channel power. Since the SINR is a scalar and requires much fewer feedback bits than the channel shape, we make the following assumption:

Assumption 3: The SINR_u is perfectly known to the base station through feedback.

The same assumption is also made in [21], [22]. The effect of SINR quantization on the throughput is shown to be insignificant using numerical results in Section V.

B. Joint Scheduling and Beamforming

This section focuses on the joint scheduling and beamforming algorithm designed based on the principles of PU2RC. Having collected quantized CSI from all U users³, the base station schedules N_t users for transmission and computes their beamforming vectors. To maximize the throughput, N_t scheduled users must be selected through an exhaustive search, which is infeasible for a large user pool. Therefore, we adopt a simpler joint scheduling and beamforming algorithm. In brief, this algorithm schedules a subset of users with orthogonal quantized channel shapes, and furthermore applies these channel shapes as the scheduled users' beamforming vectors.

The joint scheduling and beamforming algorithm is elaborated as follows. First, each member of the codebook \mathcal{F} , which is a potential beamforming vector, is assigned a user with the maximum SINR. Consider an arbitrary vector, for instance $\mathbf{v}_n^{(m)}$, which is the n th member of the m th orthonormal subset $\mathcal{V}^{(m)}$ of the codebook \mathcal{F} . This vector can be the quantized channel shapes of multiple users, whose indices are grouped in a set defined as $\mathcal{I}_n^{(m)} = \{1 \leq u \leq U : \hat{\mathbf{s}}_u = \mathbf{v}_n^{(m)}\}$ where $\hat{\mathbf{s}}_u$ is the u th user's quantized channel shape given in (3). From (3), $\mathcal{I}_n^{(m)}$ can be equivalently defined as

$$\mathcal{I}_n^{(m)} = \left\{ 1 \leq u \leq U \mid d(\mathbf{s}_u, \mathbf{v}_n^{(m)}) < d(\mathbf{s}_u, \mathbf{v}) \ \forall \mathbf{v} \in \mathcal{F} \text{ and } \mathbf{v} \neq \mathbf{v}_n^{(m)} \right\}. \quad (6)$$

Among the users in $\mathcal{I}_n^{(m)}$, $\mathbf{v}_n^{(m)}$ is associated with the one providing the maximum SINR, which is feasible since the SNRs are known to the base station through feedback. The index $(i_n^{(m)})$ and SINR $(\xi_n^{(m)})$ of this user associated with $\mathbf{v}_n^{(m)}$ can be written as

$$i_n^{(m)} = \arg \max_{u \in \mathcal{I}_n^{(m)}} \text{SINR}_u \quad \text{and} \quad \xi_n^{(m)} = \max_{u \in \mathcal{I}_n^{(m)}} \text{SINR}_u, \quad (7)$$

³For simplicity, we assume that the number of feedback bits per user is limited but not the total number of feedback bits from all users. Nevertheless, the sum feedback from all users can be reduced by allowing only a small subset of users for feedback, which is an topic addressed in a separate paper [36].

where the index set $\mathcal{I}_n^{(m)}$ and the function SINR_u are expressed respectively in (6) and (5). In the event that $\mathcal{I}_n^{(m)} = \emptyset$, the vector $\mathbf{v}_n^{(m)}$ is associated with no user and the maximum SINR $\xi_n^{(m)}$ in (7) is set as zero. Second, the orthonormal subset of the codebook that maximizes throughput is chosen, whose index is $m^* = \arg \max_{1 \leq m \leq M} \sum_{n=1}^{N_t} \log \left(1 + \xi_n^{(m)} \right)$. Thereby, the users associated with this chosen subset, specified by the indices $\left\{ i_n^{(m^*)} \mid 1 \leq n \leq N_t \right\}$, are scheduled for simultaneous transmission using beamforming vectors from the (m^*) th orthonormal subset.

The above scheduling algorithm does not guarantee that the number of scheduled users is equal to N_t , the spatial degrees of freedom. For a small user pool, the number of scheduled users is smaller than N_t . This is desirable because it is unlikely to find N_t simultaneous users with close-to-orthogonal channels in a small user pool. In this case, having fewer scheduled users than N_t reduces interference and leads to higher throughput. As the total number of users increases, the number of scheduled users converges to N_t . Numerical results on the average number of scheduled users for PU2RC are presented in Section V.

Based on the preceding algorithm for joint beamforming and scheduling, the ergodic throughput for PU2RC is given as

$$R = \mathbb{E} \left[\max_{1 \leq m \leq M} \sum_{n=1}^{N_t} \log \left(1 + \max_{u \in \mathcal{I}_n^{(m)}} \text{SINR}_u \right) \right] \quad (8)$$

where SINR_u is given in (5). The scaling of R with the number of users U as $U \rightarrow \infty$ is analyzed in Section IV.

IV. ASYMPTOTIC THROUGHPUT SCALING

In this section, we derive the scaling laws of the PU2RC throughput for an asymptotically large number of users. Auxiliary results required in the analysis are first presented in Section IV-A. Three SNR regimes, namely *normal*, *interference-limited*, and *noise-limited* regimes, are considered in Section IV-B to IV-D, respectively. Finally, numerical results showing how the asymptotic throughput scaling laws apply in the non-asymptotic regime are presented in Section IV-E. The asymptotic throughput scaling laws derived in this section for downlink SDMA are observed to be identical to those for uplink SDMA [31]. This suggests duality between uplink and downlink SDMA in terms of asymptotic throughput.

A. Auxiliary Results

Two auxiliary results are provided in this section. In Section IV-A.1, the theory of uniform convergence in the weak law of large numbers is discussed, which is an important tool for the subsequent asymptotic throughput analysis. The other useful result related to the channel-shape quantization error is presented in Section IV-A.2.

1) *Uniform Convergence in the weak law of large numbers:* In this section, a lemma on the uniform convergence in the weak law of large numbers [30] is obtained by generalizing [37, Lemma 4.8] from \mathbb{R}^3 to \mathbb{C}^{N_t} . This lemma is useful for analyzing the number of users whose channel shapes lie in one of a set of congruent disks on the surface of a unit hyper-sphere in \mathbb{C}^{N_t} .

Lemma 1 (Gupta and Kumar): Consider U random points uniformly distributed on the surface of a unit hyper-sphere in \mathbb{C}^{N_t} and N disks on the sphere surface that have equal volume denoted as A . Let T_n denote the number of points belong to the n th disk. For every $\tau_1, \tau_2 > 0$

$$\Pr \left(\sup_{1 \leq n \leq N} \left| \frac{T_n}{U} - A \right| \leq \tau_1 \right) > 1 - \tau_2, \quad U \geq U_o \quad (9)$$

where

$$U_o = \max \left\{ \frac{3}{\tau_1} \log \frac{16c}{\tau_2}, \frac{4}{\tau_1} \log \frac{2}{\tau_2} \right\} \quad (10)$$

and c is a constant.

Proof: See Appendix I. □

2) *Quantization Error of Channel Shape:* The complementary CDF of the CSI quantization error ϵ is analyzed as follows. As defined in Section III-A, $\epsilon = \sin^2(\angle(\hat{\mathbf{s}}, \mathbf{s}))$ where \mathbf{s} and $\hat{\mathbf{s}}$ are the original and the quantized channel shapes of an arbitrary user. From the quantization function in (3), the complementary CDF of ϵ is

$$\Pr(\epsilon \geq \delta) = \Pr \left(\mathbf{s} \notin \bigcup_{\mathbf{v} \in \mathcal{F}} B_\delta(\mathbf{v}) \right), \quad (11)$$

where $0 \leq \delta \leq 1$ and $B_\delta(\mathbf{v}) = \{\mathbf{s} \in \mathbb{O}^{N_t} : |\mathbf{s}^\dagger \mathbf{v}|^2 \leq \delta\}$ is a sphere cap on the unit sphere \mathbb{O}^{N_t} . The CDF of ϵ for $0 \leq \delta \leq \frac{1}{2}$ has the simple expression as given in the following lemma, but the derivation of CDF for $\frac{1}{2} \leq \delta \leq 1$ is difficult because the sphere caps $\{B_\delta(\mathbf{v}) : \mathbf{v} \in \mathcal{F}\}$ overlap.

Lemma 2: The complementary CDF of ϵ , $\Pr(\epsilon \geq \delta)$, for $0 \leq \delta \leq \frac{1}{2}$ is given as

$$\Pr(\epsilon \geq \delta) = [1 - N_t \delta^{N_t-1}]^M, \quad 0 \leq \delta \leq \frac{1}{2}, \quad (12)$$

where M is the number of orthonormal bases in the quantization codebook \mathcal{F} . In addition, $\Pr(\epsilon \geq \delta) \leq (1 - \delta^{N_t-1})^M \quad \forall 0 \leq \delta \leq 1$.

Proof: See Appendix II. □

Next, the following lemma provides an upper-bound for the quantity $\mathbb{E}[-\log \epsilon]$, which is useful for the throughput analysis in the sequel. The derivation of this result uses Lemma 2 and [27, Lemma 4].

Lemma 3: Given a codebook of M orthonormal bases, the following inequality holds

$$\frac{\log M}{(N_t - 1)P_\alpha} + \frac{\log N_t}{N_t - 1} \leq \mathbb{E}[-\log \epsilon] \leq \frac{\log M + 1}{(N_t - 1)P_\alpha} + \frac{\log N_t}{N_t - 1} \quad (13)$$

where ϵ is the channel-shape quantization error and

$$P_\alpha = 1 - \left[1 - N_t 2^{-(N_t-1)}\right]^M. \quad (14)$$

Proof: See Appendix III. \square

B. Normal SNR Regime

In this section, the throughput scaling law of PU2RC is analyzed for the normal SNR regime, where the SINR and throughput are given respectively in (5) and (8). As shown in the sequel, in the normal SNR regime, the throughput of PU2RC scales double logarithmically with the number of users and linearly with the number of antennas. This throughput scaling law is identical to those for ZF-SDMA [20] and OSDMA [22]. Therefore, these algorithms all achieve optimal multiuser diversity gain.

The procedure for deriving the throughput scaling law for PU2RC is to first obtain an upper-bound for the throughput scaling factor and second prove its achievability. The achievability proof uses Lemma 1 on the uniform convergence in the weak law of large numbers. The above procedure is also adopted for the throughput analysis for other regimes in subsequent sections.

For the normal SNR regime, the throughput scaling factor for PU2RC is upper bounded as shown in the following lemma.

Lemma 4: In the normal SNR regime, the throughput scaling factor for PU2RC is upper bounded as

$$\lim_{U \rightarrow \infty} \frac{R}{N_t \log \log U} \leq 1. \quad (15)$$

Proof: See Appendix IV. \square

Next, the upper-bound in (15) is shown to be achievable. Thereby, the throughput scaling law of PU2RC in the normal SNR regime is obtained as shown in the following proposition.

Proposition 1: In the normal SNR regime, the throughput scaling law for PU2RC is

$$\lim_{U \rightarrow \infty} \frac{R}{N_t \log \log U} = 1. \quad (16)$$

Proof: See Appendix V. \square

The proof uses Lemma 1 on the uniform convergence in the weak law of the large number. As shown in the proof, to achieve the throughput scaling law in (16), the quantization errors and channel power of scheduled users must scale with the number of users U as $\frac{1}{\log U}$ and $\log U$, respectively. This suggests that a scheduler for the normal SNR regime should schedule users with both small quantization errors and large channel power as U increases.

C. Interference-Limited Regime

In this section, the throughput scaling law of PU2RC is analyzed for the interference-limited regime where interference dominates over noise. By omitting the noise term, the SINR in (5) for the interference-limited regime reduces to

$$\text{SINR}_u^{(\alpha)} = \frac{1}{\epsilon_u} - 1 \quad (17)$$

where the superscript (α) identifies the interference-limited regime. By substituting (17) into (8), the throughput for the interference-limited regime is written as

$$R^{(\alpha)} = E \left[\max_{1 \leq m \leq M} \sum_{n=1}^{N_t} \log \left(\max_{u \in \mathcal{I}_n^{(m)}} \frac{1}{\epsilon_u} \right) \right]. \quad (18)$$

The scaling law of $R^{(\alpha)}$ with U is obtained as follows.

The upper-bound of the scaling factor of $R^{(\alpha)}$ with U is shown in the following lemma.

Lemma 5: In the interference limited regime, the throughput scaling factor is upper bounded as

$$\lim_{U \rightarrow \infty} \frac{R^{(\alpha)}}{\frac{N_t}{N_t-1} \log U} \leq 1. \quad (19)$$

Proof: See Appendix VI. □

This proof uses Lemma 3 in Section IV-A.2.

Next, the equality in (19) is shown to be achievable. The main result of this section is summarized in the following proposition.

Proposition 2: In the interference-limited regime, the throughput scaling law for PU2RC is

$$\lim_{U \rightarrow \infty} \frac{R^{(\alpha)}}{\frac{N_t}{N_t-1} \log U} = 1. \quad (20)$$

Proof: See Appendix VII. □

Again, this proof makes use of Lemma 1 on the uniform convergence in the weak law of large numbers. By comparing Propositions 1 and 2, the throughput scales as $\frac{N_t}{N_t-1} \log U$ in the interference-limited regime but $N_t \log U$ otherwise. The reason for this difference is that the asymptotic throughput is determined by the channel power (ρ) in the normal SNR and noise-limited regimes, but by the CSI quantization errors (ϵ) of scheduled users in the interference-limited regime. In the normal SNR and noise-limited regimes, the asymptotic throughput can be written as $N_t \mathbb{E}[\log \rho]$, where ρ scales as $\log U$ due to multiuser diversity gain. In the interference-limited regime, the asymptotic throughput is given as $N_t \mathbb{E}[-\log \epsilon]$ and the scaling law of ϵ is $U^{-\frac{1}{N_t-1}}$.

A few remarks are in order.

- 1) The linear scaling factor in (20), namely $N_t/(N_t - 1)$, is smaller than N_t , which is the number of available spatial degrees of freedoms. This indicates the loss in multiplexing gain for $N_t \geq 3$ in the interference-limited regime. Such loss is not observed in the normal SNR (cf. Proposition 1) or noise-limited (cf. Proposition 3) regimes.
- 2) In the interference-limited regime, scheduling users with small channel-shape quantization errors is sufficient for ensuring optimal throughput scaling. The reason is that the SINR in (17) depends only on the quantization error.
- 3) In the interference-limited regime, the throughput scaling law for PU2RC is identical to that for ZF-SDMA [20, Theorem 2]⁴.

D. Noise-Limited Regime

In this section, the throughput scaling law of PU2RC in the noise-limited regime is analyzed, where noise dominates over multiuser interference. By removing the interference term ($\gamma\rho_u\epsilon_u$) in (5), the SINR for the noise-limited regime is given as

$$\text{SINR}_u^{(\beta)} = \gamma\rho_u(1 - \epsilon_u) \quad (21)$$

where the superscript (β) specifies the noise-limited regime. By substituting (21) into (8), the corresponding throughput is written as

$$R^{(\beta)} = E \left\{ \max_{1 \leq m \leq M} \sum_{n=1}^{N_t} \log \left[1 + \max_{u \in \mathcal{I}_n^{(m)}} \gamma\rho_u(1 - \epsilon_u) \right] \right\}. \quad (22)$$

The scaling law of $R^{(\beta)}$ with U for $U \rightarrow \infty$ is obtained as shown in the following proposition.

Proposition 3: In the noise-limited regime, the throughput for PU2RC scales as follows

$$\lim_{U \rightarrow \infty} \frac{R^{(\beta)}}{N_t \log \log U} = 1. \quad (23)$$

Proof: See Appendix VIII. □

By comparing Proposition 1 and 3, the throughput scaling laws are observed to be identical for both the normal SNR and noise-limited regimes. Moreover, as reflected in the proof, to achieve the optimal throughput scaling law, scheduled users in the noise-limited regime are required to have channel power scaling as $\log U$ and quantization errors smaller than a constant d_{\min} defined in (42). Thus, for the noise-limited regime, channel power is a more important scheduling criterion than quantization errors.

⁴Note that [20, (45)] gives the throughput scaling law for a single scheduled user. Multiplication of this result with N_t gives the identical throughput scaling law for PU2RC as shown in Proposition 2.

E. Non-Asymptotic Regimes

In preceding sections, the throughput scaling laws for PU2RC are derived for different asymptotic regimes characterized by an asymptotically large number of users ($U \rightarrow \infty$). In this section, these asymptotic scaling laws are compared with their counterparts in the non-asymptotic regimes corresponding to a finite number of users ($U < \infty$). The purpose of such a comparison is to evaluate the usefulness of the asymptotic results derived in previous section for characterizing the throughput of practical PU2RC systems.

For this purpose, Fig. 2 shows the throughput versus number of users curves for the SNR values of $\{0, 5, 30\}$ dB, corresponding respectively to the noise-limited, the normal SNR and the interference-limited regimes. The range of the number of users is $1 \leq U \leq 140$, the number of transmit antennas is $N_t = 2$ and the codebook size is $N = 16$. The above curves present the PU2RC throughput scaling laws in the non-asymptotic regimes. Also plotted in Fig. 2 are the curves defined by the asymptotic throughput scaling law $\frac{N_t}{N_t-1} \log U$ for the interference-limited regime (cf. Proposition 2) and $N_t \log \log U$ for both the normal SNR and the noise-limited regimes (cf. Proposition 1 and 3). As observed from Fig. 2, as the number of users increases, the non-asymptotic curve for SNR = 30 dB becomes parallel to the curve following the asymptotic throughput scaling law $\frac{N_t}{N_t-1} \log U$. Likewise, the non-asymptotic curves for SNR = 0 dB and 5 dB have the same slopes as the corresponding asymptotic curve defined by $N_t \log \log U$. Therefore, the asymptotic throughput scaling laws also hold in the non-asymptotic regimes. Note that the gaps between the asymptotic and non-asymptotic curves are throughput constant factors that become insignificant in the asymptotic regimes ($U \rightarrow \infty$).

V. NUMERICAL RESULTS

In this section, various numerical results are presented. In Section V-A, the effect of increasing channel shape feedback on throughput is investigated. In Section V-B, for an increasing number of users, the throughput of PU2RC is evaluated against that of ZF-SDMA in [20] as well as the upper bound achieved by dirty paper coding (DPC) and multiuser water filling [38]. For simplicity, Assumption 3 is made and thus the SINR feedback is assumed perfect for all algorithms in comparison. In Section V-C, the capacity loss due to the SINR quantization is characterized.

A. Effect of Increasing Channel Shape Feedback

For PU2RC, increasing channel shape feedback does not necessarily lead to higher throughput as shown in Fig. 3. In Fig. 3, the curves of PU2RC throughput versus the number of users U are plotted for different codebook sizes N . The SNR is 5 dB and the number of transmit antennas is $N_t = 4$. Fig. 3(a) and Fig. 3(b) show the small ($1 \leq U \leq 50$) and the large user ranges ($1 \leq U \leq 200$), respectively. As observed

from Fig. 3(a), in the range of $4 \leq U \leq 22$, increasing N decreases the throughput. The reason is that a larger codebook size divides the user pool because each user is associated with only one codebook vector (cf. Section III-B). Consequently, increasing the codebook size reduces the probability of finding scheduled users with large channel gains and also associated with the same orthonormal basis in the codebook. Nevertheless, such an adverse effect of increasing the codebook size diminishes as the number of users increases. As shown in Fig. 3, for $U \geq 70$, a larger codebook size results in higher throughput. The above results motivate the need for choosing an optimal codebook size for a given number of users.

B. Comparison with ZF-SDMA and Dirty Paper Coding

Presently, PU2RC and ZF-SDMA [4], [6], [20] are two main solutions for multiuser MIMO downlink for 3GPP-LTE. In this section, their performance is compared using numerical results. Moreover, the throughput of PU2RC is evaluated against the upper-bound achieved by dirty paper coding.

In Fig. 4, the throughput of PU2RC is compared with that of ZF-SDMA for an increasing number of users. The number of transmit antenna is $N_t = 4$ and the SNR is 5 dB. Moreover, the codebook sizes $N = \{4, 8, 16, 32\}$ for channel shape quantization are considered. As in [20], the threshold 0.25 is applied in the greedy-search scheduling for ZF-SDMA. Fig. 4(a) and Fig. 4(b) show respectively the small ($1 \leq U \leq 35$) and the large ($1 \leq U \leq 200$) user ranges. As observed from Fig. 4(a), for a given codebook size (either $N = 16$ or $N = 64$), PU2RC achieves higher throughput than ZF-SDMA for a relative large number of users but the reverse holds for a smaller user pool. Specifically, in Fig. 4(a), the throughput curves for PU2RC and ZF-SDMA cross at $U = 19$ for $N = 16$ and at $U = 27$ for $N = 64$. For a sufficiently large number of users, PU2RC always outperforms ZF-SDMA in terms of throughput as shown in Fig. 4(b). Furthermore, compared with ZF-SDMA, PU2RC is found to be more robust against CSI quantization errors. For example, as observed from Fig. 4(b), for $U = 100$, the throughput loss for PU2RC due to the decrease of the codebook size from $N = 64$ to $N = 16$ is 0.3 bps/Hz but that for ZF-SDMA is 1.5 bps/Hz. The above observations are explained shortly. In summary, these observations suggest that PU2RC is preferred to ZF-SDMA for a large user pool but not for a small one.

To explain the observations from Fig. 4, the average numbers of scheduled users for PU2RC and ZF-SDMA are compared in Fig. 5 for an increasing number of users. It can be observed from Fig. 5 that PU2RC tends to schedule more users than ZF-SDMA. First, for a small number of users, interference between scheduled users can not be effectively suppressed by scheduling, and hence more simultaneous users result in smaller throughput. This explains the observation from Fig. 4(a) that PU2RC achieves lower throughput than ZF-SDMA due to more scheduled users. Second, for a large user pool, the channel vectors of scheduled users are close-to-orthogonal and interference is negligible. Therefore, a larger number of scheduled users leads to

higher throughput. For this reason, PU2RC outperforms ZF-SDMA for a large number of users as observed from Fig. 4(b). Last, with respect to ZF-SDMA, the better robustness of PU2RC against CSI quantization errors is mainly due to the joint beamforming and scheduling (cf. Section III-B). Note that beamforming and scheduling for ZF-SDMA are performed separately [20].

Fig. 6 compares the throughput of PU2RC and ZF-SDMA for an increasing SNR. The number of transmit antennas is $N_t = 4$ and the codebook size is $N = 64$. As observed from Fig. 6, for the number of users $U = 20$, PU2RC achieves lower throughput than ZF-SDMA over the range of SNR under consideration ($0 \leq \text{SNR} \leq 20$ dB). Nevertheless, for larger numbers of users ($U = 40$ or 80), PU2RC outperforms ZF-SDMA for a subset of the SNRs. Specifically, the throughput versus SNR curves for PU2RC and ZF-SDMA crosses at SNR=7 dB for $U = 40$ and at SNR=18 dB for $U = 80$. The above results suggest that in the practical range of SNR, PU2RC is preferred to ZF-SDMA only if the user pool is sufficiently large.

Fig. 7 compares the throughput of PU2RC with an upper bound achieved by *dirty paper coding* (DPC) and multiuser iterative water-filling [38]. A smaller number of antennas $N_t = 2$ is chosen to reduce the high computational complexity of iterative water-filling for a large number of users. Hence, each user has a 2×1 multiple-input-single-output (MISO) channel. Moreover, SNR = 5 dB and the channel shape codebook size is $N = \{2, 4, 8, 16\}$. As observed from Fig. 7, the gap between the throughput of PU2RC and its upper bound narrows as the number of users U or the codebook size N increases. At $U = 200$ and $N = 16$, PU2RC achieves about 85% of the sum capacity of DPC.

C. Effect of SINR Quantization

In this section, using numerical results, a small number of bits for SINR feedback is found sufficient for making the capacity loss due to SINR quantization negligible.

For PU2RC, Fig. 8 compares the cases of perfect and quantized SINR feedback. For quantizing SINR, a scalar quantizer using a squared-error distortion function is employed [32]. Moreover, the quantizer has a simple codebook containing evenly spaced scalars in the SINR range corresponding to a probability of 99%. The number of transmit antenna is $N_t = 4$, the SINR is 5 dB and the codebook size for channel shape quantization is $N = 16$. As observed from Fig. 8, 2 bits of SINR feedback per user causes only marginal loss in throughput with respect to the perfect SINR feedback. Such loss is negligible for 3-bit feedback. Therefore, a few bits of SINR feedback from each user is almost as good as the perfect case, which justifies Assumption 3.

VI. CONCLUSION

This paper presents asymptotic throughput scaling laws for SDMA with orthogonal beamforming known as PU2RC for different SNR regimes. In the interference limited regime, the throughput of PU2RC is shown

to scale logarithmically with the number of users but does not increase with the number of antennas. In the normal SNR or noise-limited regimes, the throughput of PU2RC is found to scale double logarithmically with the number of users and linearly with the number of antennas at the base station. Numerical results showed that PU2RC can achieve significant gains in throughput with respect to ZF-SDMA for the same amount of CSI feedback.

This paper focuses on the scheduling criterion of maximizing throughput. The design and performance analysis of PU2RC based on the criterion of proportional fairness is a topic under investigation. Furthermore, the optimal design for PU2RC for the non-asymptotic regime of the user pool remains as an open issue.

APPENDIX I

PROOF OF LEMMA 1

Lemma 4.8 in [37] can be generalized from \mathbb{R}^3 to \mathbb{C}^{N_t} as follows. [37, Lemma 4.8] concerns N congruent disks on the surface of a sphere in \mathbb{R}^3 , and its derivation relies on two results: the first one is the *stereographic projection* [39] that one-to-one maps a point on the surface of the sphere to a point on a plane both in \mathbb{R}^3 ; the second is that the Vapnik-Chervonenkis dimension of a set of disks on a plane in \mathbb{R}^3 is three [37]. A unit hyper-sphere in \mathbb{C}^{N_t} can be treated as one in \mathbb{R}^{2N_t} [35]. Thereby, the *stereographic projection* also exists between a unit hyper-sphere and a hyper-plane in \mathbb{C}^{N_t} [40]. Next, following the same procedure as in [37, Lemma 4.6], the Vapnik-Chervonenkis dimension of a set of disks on a hyper-plane in \mathbb{C}^{N_t} is shown to be also three. Based on the two results obtained above for \mathbb{C}^{N_t} , the remaining steps for proving Lemma 1 are identical to those for [37, Lemma 4.8] and are thus omitted.

APPENDIX II

PROOF OF LEMMA 2

Since the orthonormal bases in the codebook \mathcal{F} are independently and randomly generated, the complementary CDF (11) can be equivalently expressed as

$$\Pr(\epsilon \geq \delta) = \prod_{m=1}^M \Pr(\mathbf{s} \notin \cup_{\mathbf{v} \in \mathcal{V}^{(m)}} B_\delta(\mathbf{v})), \quad (24)$$

where $\mathcal{V}^{(m)}$ denotes the m th orthonormal basis in \mathcal{F} . Given that \mathbf{s} is isotropically distributed on the unit sphere, (24) can be re-written in terms of the *volume* of sphere caps [32]

$$\Pr(\epsilon \geq \delta) = \prod_{m=1}^M \{1 - \text{vol}[\cup_{\mathbf{v} \in \mathcal{V}^{(m)}} B_\delta(\mathbf{v})]\}. \quad (25)$$

Since the sphere caps $\{B_\delta(\mathbf{v})\} \mid \mathbf{v} \in \mathcal{V}^{(m)}\}$ are non-overlapping for $\delta \leq \frac{1}{2}$ and the volume of each sphere cap is $\text{vol}[B_\delta(\mathbf{v})] = \delta^{N_t-1}$ as obtained in [22], we can obtain from (25)

$$\Pr(\epsilon \geq \delta) = \prod_{m=1}^M (1 - N_t \delta^{N_t-1}), \quad 0 \leq \delta \leq \frac{1}{2}. \quad (26)$$

The desired result in (12) follows from the last equation. Moreover, from (25) and for $\mathbf{v} \in \mathcal{F}$, $\Pr(\epsilon \geq \delta) \leq \prod_{m=1}^M \{1 - \text{vol}[B_\delta(\mathbf{v})]\} = \prod_{m=1}^M \{1 - \delta^{N_t-1}\}$, which gives the inequality in the lemma.

APPENDIX III

PROOF OF LEMMA 3

The minimum of M i.i.d. Beta $(N_t, 1)$ random variables, denoted as $\{\beta_1, \beta_2, \dots, \beta_M\}$, has the following CDF [27]

$$\Pr\left(\min_{1 \leq m \leq M} \beta_m \geq b\right) = (1 - b^{N_t-1})^M. \quad (27)$$

From (27) and Lemma 2

$$N_t^{\frac{1}{N_t-1}} \epsilon \cong \min_{1 \leq m \leq M} \beta_m, \quad \epsilon \leq \frac{1}{2} \quad (28)$$

where \cong represents equivalence in distribution. The above equivalence results in the following equality (a)

$$\begin{aligned} \mathbb{E}\left[-\log\left(N_t^{\frac{1}{N_t-1}} \epsilon\right)\right] &\leq \mathbb{E}\left[-\log\left(N_t^{\frac{1}{N_t-1}} \epsilon\right) \mid 0 \leq \epsilon \leq \frac{1}{2}\right] \\ &\stackrel{(a)}{=} \mathbb{E}\left[-\log\left(\min_{1 \leq m \leq M} \beta_m\right) \mid 0 \leq \min_{1 \leq m \leq M} \beta_m \leq \frac{1}{2} N_t^{\frac{1}{N_t-1}}\right] \\ &\leq \frac{\mathbb{E}[-\log(\min_m \beta_m)]}{\Pr\left(0 \leq \min_m \beta_m \leq \frac{1}{2} N_t^{\frac{1}{N_t-1}}\right)}. \end{aligned} \quad (29)$$

As shown in [27, Lemma 4]

$$\frac{\log M}{N_t - 1} \leq \mathbb{E}\left[-\log\left(\min_m \beta_m\right)\right] \leq \frac{\log M + 1}{N_t - 1}. \quad (30)$$

By combining (27), (29), and (30), the desired inequality follows.

APPENDIX IV

PROOF OF LEMMA 4

From (5) and (8)

$$\begin{aligned} R &= E \left[\max_{1 \leq m \leq M} \sum_{n=1}^{N_t} \log \left(\max_{u \in \mathcal{I}_n^{(m)}} \frac{1 + \gamma \rho_u}{1 + \gamma \rho_u \epsilon_u} \right) \right] \\ &\leq E \left[\max_{1 \leq m \leq M} \sum_{n=1}^{N_t} \log \left(1 + \gamma \max_{u \in \mathcal{I}_n^{(m)}} \rho_u \right) \right] \end{aligned} \quad (31)$$

$$\begin{aligned} &\leq E \left[\sum_{n=1}^{N_t} \log \left(1 + \gamma \max_{1 \leq m \leq M} \max_{u \in \mathcal{I}_n^{(m)}} \rho_u \right) \right] \\ &= N_t E \left[\log \left(1 + \gamma \max_{1 \leq u \leq U} \rho_u \right) \right]. \end{aligned} \quad (32)$$

The following result is well-known from extreme value theory (see e.g. [22, (A10)])

$$\Pr \left(\left| \max_{1 \leq u \leq U} \rho_u - \log U \right| < O(\log \log U) \right) > 1 - O \left(\frac{1}{\log U} \right). \quad (33)$$

From (33) and (32)

$$\begin{aligned} R &\leq N_t E \{ \log [1 + \gamma \log U - \gamma O(\log \log U)] \} \Pr \left(\max_{1 \leq u \leq U} \rho_u \leq \log U - O(\log \log U) \right) + \\ &\quad N_t E \left[\log \left(1 + \gamma \sum_{u=1}^U \rho_u \right) \right] O \left(\frac{1}{\log U} \right) \\ &\stackrel{(a)}{\leq} N_t E \{ \log [1 + \gamma \log U - \gamma O(\log \log U)] \} + N_t \log (1 + \gamma N_t U) O \left(\frac{1}{\log U} \right) \end{aligned} \quad (34)$$

where (a) is obtained by using Jensen's inequality. The desired inequality follows from (34).

APPENDIX V

PROOF OF PROPOSITION 1

Define a set of disks on the unit hyper-sphere as

$$\mathcal{B}_n^{(m)}(d) = \left\{ \mathbf{s} \in \mathbb{C}^{N_t} \mid \|\mathbf{s}\|^2 = 1, 1 - |\mathbf{s}^\dagger \mathbf{v}_n^{(m)}|^2 \leq d \right\} \quad 1 \leq m \leq M, 1 \leq n \leq N_t \quad (35)$$

where d is the radius of $\mathcal{B}_n^{(m)}(d)$. Furthermore, define the user index sets

$$\hat{\mathcal{I}}_n^{(m)} = \left\{ 1 \leq u \leq U \mid \mathbf{s}_u \in \mathcal{B}_n^{(m)} \left(\frac{1}{\log U} \right) \right\} \quad 1 \leq m \leq M, 1 \leq n \leq N_t \quad (36)$$

where the disk $\mathcal{B}_n^{(m)}$ is defined in (35). By applying Lemma 1 with $\tau_1 = \tau_2 = A = \frac{1}{2(\log U)^{N_t-1}}$, we obtain that

$$\Pr \left(|\hat{\mathcal{I}}_n^{(m)}| \geq \frac{U}{(\log U)^{N_t-1}} \right) > 1 - \frac{1}{2(\log U)^{N_t-1}} \quad \forall U > U_o \quad (37)$$

where U_o is in (10). Let U_1 denote a sufficiently large integer such that $\hat{\mathcal{I}}_n^{(m)} \subset \mathcal{I}_n^{(m)}$. From (8) and (5) and by replacing $\mathcal{I}_n^{(m)}$ with $\hat{\mathcal{I}}_n^{(m)}$

$$\begin{aligned} R &\geq E \left[\sum_{n=1}^{N_t} \log \left(\max_{u \in \hat{\mathcal{I}}_n^{(m)}} \frac{1 + \gamma \rho_u}{1 + \gamma \rho_u \epsilon_u} \right) \right], \quad U \geq U_1 \\ &\stackrel{(a)}{\geq} E \left[\sum_{n=1}^{N_t} \log \left(\max_{u \in \hat{\mathcal{I}}_n^{(m)}} \frac{1 + \gamma \rho_u}{1 + \gamma \rho_u \frac{1}{\log U}} \right) \right], \quad U \geq U_1 \\ &\geq E \left[\sum_{n=1}^{N_t} \log \left(\frac{1 + \gamma \max_{u \in \hat{\mathcal{I}}_n^{(m)}} \rho_u}{1 + \frac{\gamma}{\log U} \max_{u \in \hat{\mathcal{I}}_n^{(m)}} \rho_u} \right) \right], \quad U \geq U_1 \end{aligned} \quad (38)$$

where the inequality in (a) holds because $u \in \hat{\mathcal{I}}_n^{(m)} \Rightarrow \epsilon_u \leq \frac{1}{\log U}$ according to the definition in (36). From (37) and (38)

$$\begin{aligned} R &\geq E \left[\sum_{n=1}^{N_t} \log \left(\frac{1 + \gamma \max_{u \in \hat{\mathcal{I}}_n^{(m)}} \rho_u}{1 + \frac{\gamma}{\log U} \max_{u \in \hat{\mathcal{I}}_n^{(m)}} \rho_u} \right) \mid |\hat{\mathcal{I}}_n^{(m)}| \geq \frac{U}{(\log U)^{N_t-1}} \right] \times \\ &\quad \left[1 - \frac{1}{2 (\log U)^{N_t-1}} \right] \quad \forall U > \max(U_1, U_o). \end{aligned}$$

From the last inequality and (33),

$$\begin{aligned} R &\geq N_t \mathbb{E} \left[\log \left(1 + \frac{\log \tilde{U} - O(\log \log \tilde{U})}{1/\gamma + [\log \tilde{U} + O(\log \log \tilde{U})] \frac{1}{\log U}} \right) \right] \left(1 - \frac{1}{2 (\log U)^{N_t-1}} \right) \times \\ &\quad \left[1 - O \left(\frac{1}{\log U} \right) \right]^{N_t}, \quad \forall U > \max(U_1, U_o) \end{aligned}$$

where $\tilde{U} = \frac{U}{(\log U)^{N_t-1}}$. It follows from the last inequality that

$$\lim_{U \rightarrow \infty} \frac{R}{N_t \log \log U} \geq 1. \quad (39)$$

The desired result is obtained by combining (39) and Lemma 4.

APPENDIX VI

PROOF OF LEMMA 5

From (18)

$$\begin{aligned} R^{(a)} &\leq E \left[\sum_{n=1}^{N_t} -\log \left(\min_{1 \leq m \leq M} \min_{u \in \mathcal{I}_n^{(m)}} \epsilon_u \right) \right] \\ &= N_t E \left[-\log \left(\min_{1 \leq u \leq U} \epsilon_u \right) \right]. \end{aligned} \quad (40)$$

In the above equation, $\min_{1 \leq u \leq U} \epsilon_u$ follows the same distribution as the quantization error for an enlarged codebook having MU orthonormal bases. Therefore, from (40) and Lemma 3

$$R^{(a)} \leq \frac{N_t}{N_t - 1} \left\{ \frac{\log U + \log M + 1}{1 - [1 - N_t 2^{-(N_t-1)}]^{MU}} + \log N_t \right\}. \quad (41)$$

The desired upper bound of the throughput scaling factor follows from the last inequality. Note that $\left\{ 1 - [1 - N_t 2^{-(N_t-1)}]^{MU} \right\} \rightarrow 1$ as $U \rightarrow \infty$.

APPENDIX VII

PROOF OF PROPOSITION 2

Define the minimum distance of the codebook \mathcal{F} as

$$d_{\min} = \min_{\mathbf{v}, \mathbf{v}' \in \mathcal{F}} \frac{1 - |\mathbf{v}^\dagger \mathbf{v}'|^2}{4}. \quad (42)$$

Moreover, similar to (36), define the index set of the users in the disk $\mathcal{B}_n^{(m)}(d_{\min})$ (cf. (35)) as

$$\mathcal{T}_n^{(m)} = \left\{ 1 \leq u \leq U \mid \mathbf{s}_u \in \mathcal{B}_n^{(m)}(d_{\min}) \right\}, \quad 1 \leq m \leq M, 1 \leq n \leq N_t. \quad (43)$$

By the definitions in (6) and (42), $\mathbf{s}_u \in \mathcal{B}_n^{(m)}(d_{\min}) \Rightarrow u \in \mathcal{I}_{m,n}$. Using this fact, a throughput lower bound follows by replacing $\mathcal{I}_{m,n}$ in (8) with $\mathcal{T}_{m,n}$

$$\begin{aligned} R^{(a)} &\geq E \left[\max_{1 \leq m \leq M} \sum_{n=1}^{N_t} \log \left(\max_{u \in \mathcal{T}_n^{(m)}} \frac{1}{\epsilon_u} \right) \right] \\ &\geq E \left[\sum_{n=1}^{N_t} \log \left(\max_{u \in \mathcal{T}_n^{(m)}} \frac{1}{\epsilon_u} \right) \right]. \end{aligned} \quad (44)$$

By applying Lemma 1 with $\tau_1 = \tau_2 = U^{-\frac{1}{2}}$ and $A = d_{\min}^{N_t-1}$, the numbers of users belonging to the index sets (36) satisfy

$$\Pr \left(\min_{m,n} |\mathcal{T}_n^{(m)}| \geq d_{\min}^{N_t-1} U - U^{\frac{1}{2}} \right) \geq 1 - U^{-\frac{1}{2}}, \quad \forall U \geq U_o \quad (45)$$

where U_o is defined in (10). From (44) and (45)

$$R^{(a)} \geq N_t E \left[-\log \left(\min_{u \in \mathcal{T}_n^{(m)}} \epsilon_u \right) \mid |\mathcal{T}_n^{(m)}| \geq d_{\min}^{N_t-1} U - U^{\frac{1}{2}} \right] \left(1 - U^{-\frac{1}{2}} \right), \quad U \geq U_o.$$

By applying Lemma 3

$$R^{(a)} \geq \frac{N_t}{N_t - 1} \left[\frac{\log M + \log d_{\min}^{N_t-1} + \log U + \log(1 - U^{-\frac{1}{2}})}{P_\alpha} + \log N_t \right] \left(1 - U^{-\frac{1}{2}} \right), \quad U \geq U_o \quad (46)$$

where P_α is modified from (14) as

$$P_\alpha = 1 - \left[1 - N_t 2^{-(N_t-1)} \right]^{M(d_{\min}^{N_t-1} U - U^{\frac{1}{2}})} \quad (47)$$

It follows from the last inequality that

$$\lim_{U \rightarrow \infty} \frac{R^{(a)}}{\frac{N_t}{N_t-1} \log U} \geq 1. \quad (48)$$

Combining (48) and (19) gives the desired throughput scaling law for the interference-limited regime.

APPENDIX VIII

PROOF OF PROPOSITION 3

From (22) and since $0 \leq \epsilon_u \leq 1$

$$R^{(\beta)} \leq \mathbb{E} \left[\max_{1 \leq m \leq M} \sum_{n=1}^{N_t} \log \left(1 + \gamma \max_{u \in \mathcal{I}_m^{(n)}} \rho_u \right) \right]. \quad (49)$$

In (31) in Appendix IV, the above upper-bound is also used for bounding the PU2RC throughput in the normal SNR regime. Therefore, the upper-bound for the throughput scaling factor as obtained in Appendix IV is also applicable for the present case, hence

$$\lim_{U \rightarrow \infty} \frac{R^{(\beta)}}{N_t \log \log U} \leq 1. \quad (50)$$

Next, the above upper bound is shown to be achievable as follows. By replacing the index set $\mathcal{I}_n^{(m)}$ in (22) with its subset $\mathcal{T}_n^{(m)}$ defined in (43)

$$\begin{aligned} R^{(\beta)} &\geq \mathbb{E} \left\{ \sum_{n=1}^{N_t} \log \left[1 + \gamma \max_{u \in \mathcal{T}_m^{(n)}} \rho_u (1 - \epsilon_u) \right] \right\} \\ &\stackrel{(a)}{\geq} \mathbb{E} \left\{ \sum_{n=1}^{N_t} \log \left[1 + \gamma(1 - d_{\min}) \max_{u \in \mathcal{T}_m^{(n)}} \rho_u \right] \right\} \\ &\stackrel{(b)}{\geq} \mathbb{E} \left\{ \sum_{n=1}^{N_t} \log \left[1 + \gamma(1 - d_{\min}) \max_{u \in \mathcal{T}_m^{(n)}} \rho_u \right] \mid |\mathcal{T}_m^{(n)}| \geq d_{\min}^{N_t-1} U - 1 \right\} \left(1 - \frac{1}{U} \right), U \geq U_o \\ &\stackrel{(c)}{\geq} N_t \mathbb{E} \left\{ \log \left[1 + \gamma(1 - d_{\min}) \log(d_{\min}^{N_t-1} U - 1) + \gamma(1 - d_{\min}) O(\log \log U) \right] \right\} \left(1 - \frac{1}{U} \right) \times \\ &\quad \left[1 - O \left(\frac{1}{\log U} \right) \right]^{N_t}, U \geq U_o. \end{aligned}$$

The inequality (a) follows from the definition of $\mathcal{T}_n^{(m)}$ in (43). The inequality (b) follows from (45). The inequality (c) is obtained by using (33). It follows from (c) that

$$\lim_{U \rightarrow \infty} \frac{R^{(\beta)}}{N_t \log \log U} \geq 1. \quad (51)$$

Combining (50) and (51) gives the desired throughput scaling law.

REFERENCES

- [1] P. Viswanath and D. Tse, "Sum capacity of the vector Gaussian broadcast channel and uplink-downlink duality," *IEEE Trans. on Info. Theory*, vol. 49, pp. 1912–21, Aug. 2003.
- [2] "IEEE 802.16e amendment: Physical and medium access control layers for combined fixed and mobile operation in licensed bands," *IEEE Standard 802.16*, 2005.
- [3] "3GPP TR 25.814: Physical layer aspects for evolved universal terrestrial radio access (release 7)," June 2006.
- [4] Motorola, Inc, "Downlink MIMO summary," in *3GPP TSG RAN WG1 # 49-bis/R1-072693*, June 2006.
- [5] Samsung Electronics, "Downlink MIMO for EUTRA," in *3GPP TSG RAN WG1 # 44/R1-060335*, Feb. 2006.
- [6] Freescale Semiconductor, "Details of zero-forcing MU-MIMO for DL EUTRA," in *3GPP TSG RAN WG1 # 48-bis/R1-071510*, Mar. 2007.
- [7] M. Costa, "Writing on dirty paper," *IEEE Trans. on Info. Theory*, vol. 29, no. 3, pp. 439 – 441, 1983.
- [8] W. Yu, D. P. Varodayan, and J. M. Cioffi, "Trellis and convolutional precoding for transmitter-based interference pre-subtraction," *IEEE Trans. on Communications*, vol. 53, pp. 1220–30, July 2005.
- [9] Q. H. Spencer, C. B. Peel, A. L. Swindlehurst, and M. Haardt, "An introduction to the multi-user MIMO downlink," *IEEE Communications Magazine*, vol. 42, pp. 60–67, Oct. 2004.
- [10] L.-U. Choi and R. Murch, "A transmit preprocessing technique for multiuser MIMO systems using a decomposition approach," *IEEE Trans. on Wireless Communications*, vol. 3, no. 1, pp. 20–24, 2004.
- [11] K.-K. Wong, R. Murch, and K. Letaief, "A joint-channel diagonalization for multiuser MIMO antenna systems," *IEEE Trans. on Wireless Communications*, vol. 2, no. 4, pp. 773–786, 2003.
- [12] Q. H. Spencer, A. L. Swindlehurst, and M. Haardt, "Zero-forcing methods for downlink spatial multiplexing in multiuser MIMO channels," *IEEE Trans. on Signal Processing*, vol. 52, no. 2, pp. 461 – 471, 2004.
- [13] G. Dimic and N. D. Sidiropoulos, "On downlink beamforming with greedy user selection: performance analysis and a simple new algorithm," *IEEE Trans. on Signal Processing*, vol. 53, pp. 3857–68, Oct. 2005.
- [14] M. Schubert and H. Boche, "Solution of the multiuser downlink beamforming problem with individual SINR constraints," *IEEE Trans. on Veh. Technol.*, vol. 53, pp. 18–28, Jan. 2004.
- [15] S. Serbetli and A. Yener, "Transceiver optimization for multiuser MIMO systems," *IEEE Trans. on Signal Processing*, vol. 52, pp. 214–226, Jan. 2004.
- [16] Y.-S. Choi, S. Alamouti, and V. Tarokh, "Complementary beamforming: new approaches," *IEEE Trans. on Communications*, vol. 54, no. 1, pp. 41–50, 2006.
- [17] R. Knopp and P. Humblet, "Information capacity and power control in single-cell multiuser communications," in *Proc., IEEE Intl. Conf. on Communications*, vol. 1, pp. 331–5, 1995.
- [18] C. Swannack, E. Uysal-Biyikoglu, and G. W. Wornell, "MIMO broadcast scheduling with limited channel state information," in *Proc., Allerton Conf. on Comm., Control, and Computing*, Sept. 2005.
- [19] T. Yoo and A. Goldsmith, "On the optimality of multiantenna broadcast scheduling using zero-forcing beamforming," *IEEE Journal on Sel. Areas in Communications*, vol. 24, pp. 528–541, Mar. 2006.
- [20] T. Yoo, N. Jindal, and A. Goldsmith, "Multi-antenna broadcast channels with limited feedback and user selection," *IEEE Journal on Sel. Areas in Communications*, vol. 25, pp. 1478–91, July 2007.

- [21] W. Choi, A. Forenza, J. G. Andrews, and R. W. Heath Jr., "Opportunistic space division multiple access with beam selection," *IEEE Trans. on Communications*, vol. 55, pp. 2371–80, Dec. 2007.
- [22] M. Sharif and B. Hassibi, "On the capacity of MIMO broadcast channels with partial side information," *IEEE Trans. on Info. Theory*, vol. 51, pp. 506–522, Feb. 2005.
- [23] Z. Shen, R. Chen, J. G. Andrews, R. W. Heath Jr., and B. L. Evans, "Low complexity user selection algorithms for multiuser MIMO systems with block diagonalization," *IEEE Trans. on Signal Processing*, vol. 54, pp. 3658–63, Sept. 2006.
- [24] D. J. Love, R. W. Heath Jr., W. Santipach, and M. L. Honig, "What is the value of limited feedback for MIMO channels?," *IEEE Comm. Mag.*, vol. 42, pp. 54–59, Oct. 2004.
- [25] D. J. Love and R. W. Heath Jr., "Feedback techniques for MIMO channels," in *MIMO Antenna Technology for Wireless Communications*, (Boca Raton, FL), CRC Press Inc, 2006.
- [26] P. Ding, D. J. Love, and M. D. Zoltowski, "On the sum rate of channel subspace feedback for multi-antenna broadcast channels," in *Proc., IEEE Globecom*, vol. 5, pp. 2699–2703, Nov. 2005.
- [27] N. Jindal, "MIMO broadcast channels with finite-rate feedback," *IEEE Trans. on Info. Theory*, vol. 52, pp. 5045–60, Nov. 2006.
- [28] H. Yin and H. Liu, "Performance of space-division multiple-access (SDMA) with scheduling," *IEEE Trans. on Wireless Communications*, vol. 1, no. 4, pp. 611–618, 2002.
- [29] C. K. Au-Yeung and D. J. Love, "On the performance of random vector quantization limited feedback beamforming in a MISO system," *IEEE Trans. on Wireless Communications*, vol. 6, pp. 458–462, Feb. 2007.
- [30] V. N. Vapnik and A. Chervonenkis, "On the uniform convergence of relative frequencies of events to their probabilities," *Theory of Probab. and its Applic.*, vol. 16, pp. 264–280, Feb. 1971.
- [31] K.-B. Huang, R. W. Heath Jr., and J. G. Andrews, "Uplink SDMA with limited feedback: Throughput scaling," *EURASIP Journal on Advances in Sig. Processing*, vol. 2008, Article ID 479357, 2008. doi:10.1155/2008/479357.
- [32] A. Gersho and R. M. Gray, *Vector Quantization and Signal Compression*. Kluwer Academic Press, 1992.
- [33] K. Zyczkowski and M. Kus, "Random unitary matrices," *J. Phys.*, vol. A27, pp. 4235–45, June 1994.
- [34] D. J. Love, R. W. Heath Jr., and T. Strohmer, "Grassmannian beamforming for multiple-input multiple-output wireless systems," *IEEE Trans. on Info. Theory*, vol. 49, pp. 2735–47, Oct. 2003.
- [35] K. K. Mukkavilli, A. Sabharwal, E. Erkip, and B. Aazhang, "On beamforming with finite rate feedback in multiple antenna systems," *IEEE Trans. on Info. Theory*, vol. 49, pp. 2562–79, Oct. 2003.
- [36] K.-B. Huang, R. W. Heath Jr., and J. G. Andrews, "SDMA with a sum feedback rate constraint," *IEEE Trans. on Signal Processing*, vol. 55, pp. 3879–91, July 2007.
- [37] P. Gupta and P. R. Kumar, "The capacity of wireless networks," *IEEE Trans. on Info. Theory*, vol. 46, pp. 388–404, Mar. 2000.
- [38] N. Jindal, W. Rhee, S. Vishwanath, S. A. Jafar, and A. Goldsmith, "Sum power iterative water-filling for multi-antenna gaussian broadcast channels," *IEEE Trans. on Info. Theory*, vol. 51, pp. 1570–80, Apr. 2005.
- [39] D. A. Brannan, M. F. Esplen, and J. J. Gray, *Geometry*. Cambridge University Press, 1999.
- [40] B. Rosenfeld, *Geometry of Lie Groups*. Springer, 1997.

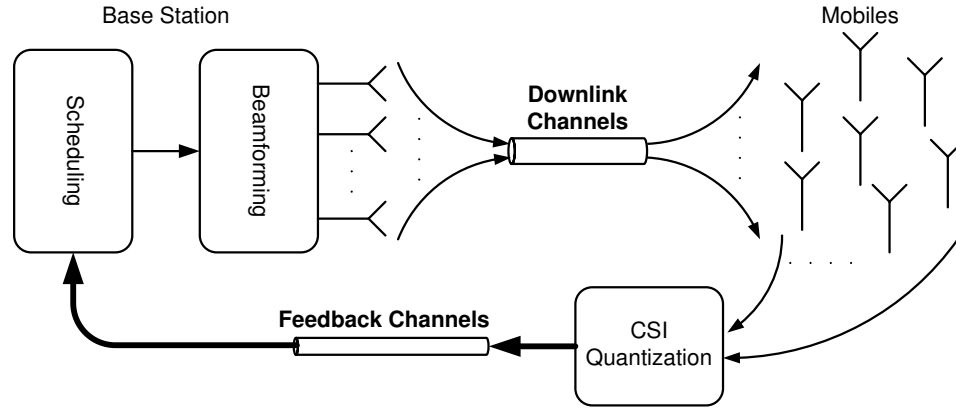


Fig. 1. Downlink system with limited feedback

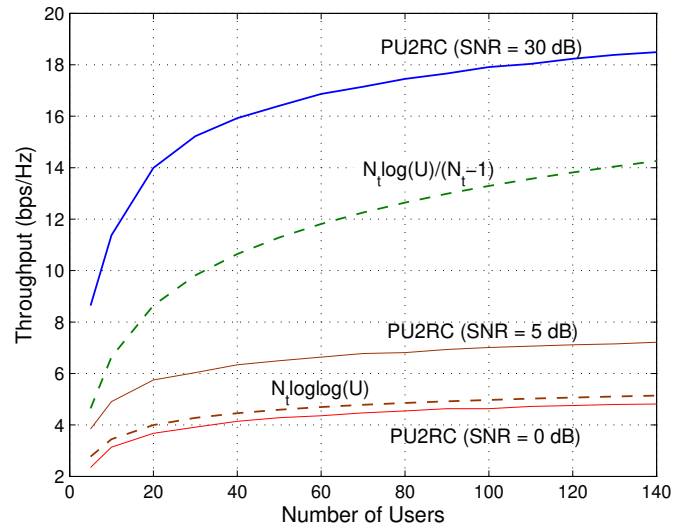
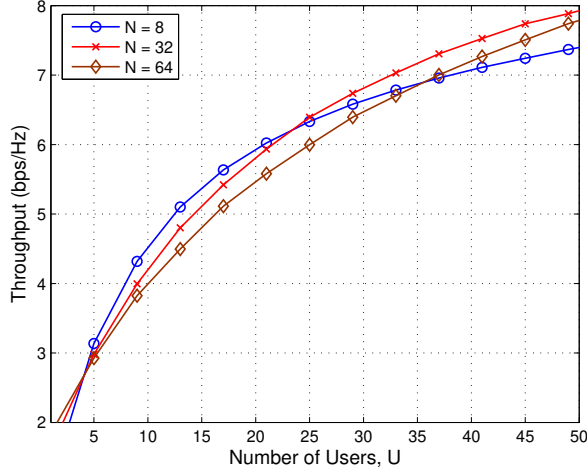
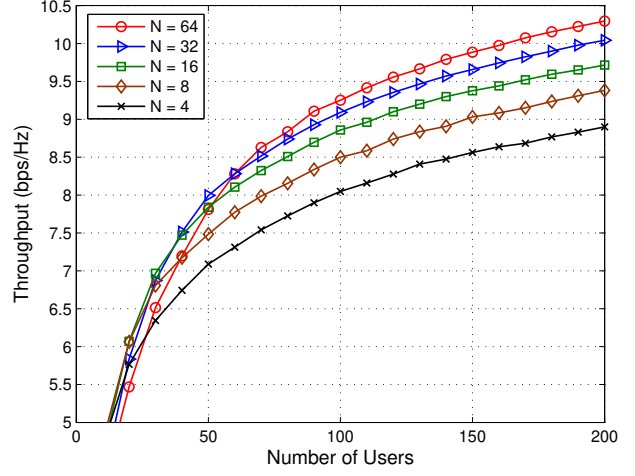


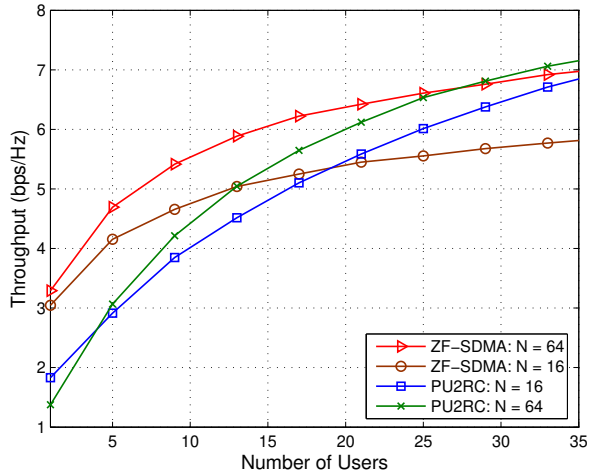
Fig. 2. Comparison between asymptotic and non-asymptotic throughput scaling laws for PU2RC for $\text{SNR} = \{0, 5, 30\}$ dB, the codebook size $N = 16$, and the number of transmit antennas $N_t = 2$.



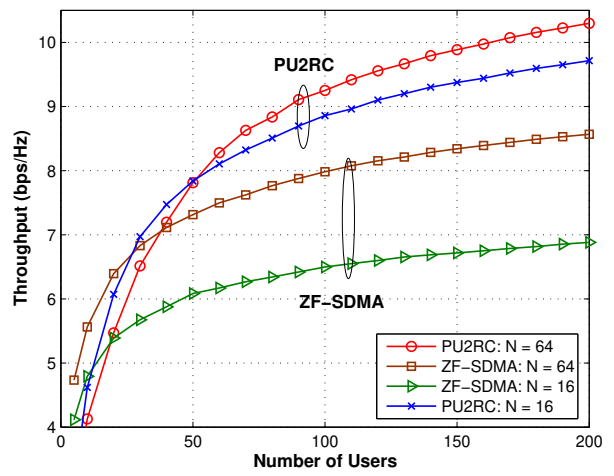
(a) Small numbers of users



(b) Large numbers of users

Fig. 3. Throughput of PU2RC for an increasing number of users U , SNR = 5 dB, and the number of transmit antennas $N_t = 4$.

(a) Small Numbers of Users



(b) Large Numbers of Users

Fig. 4. Throughput comparison between PU2RC and ZF-SDMA for an increasing number of users U , SNR = 5 dB, and the number of transmit antennas $N_t = 4$.

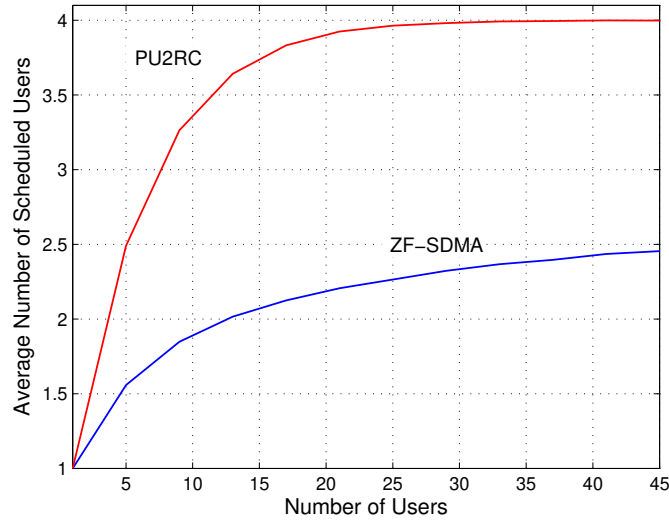


Fig. 5. The average numbers of scheduled users for PU2RC and ZF-SDMA for SNR = 5 dB, and the number of transmit antennas $N_t = 4$.

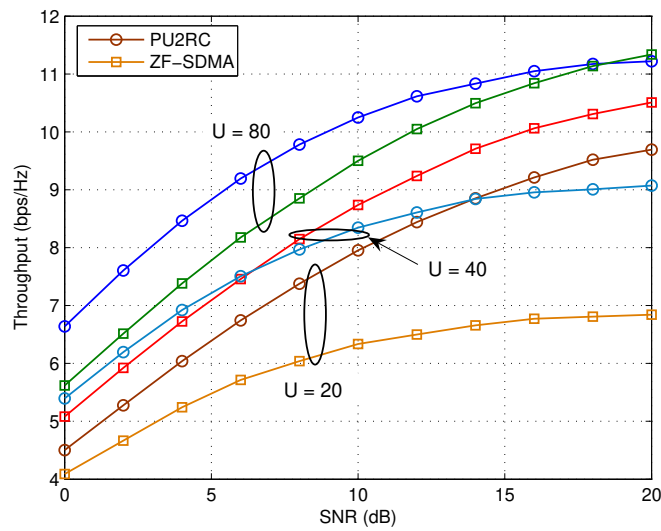


Fig. 6. Throughput comparison between PU2RC and ZF-SDMA for an increasing number SNR; The codebook size $N = 64$ and the number of transmit antennas $N_t = 4$.

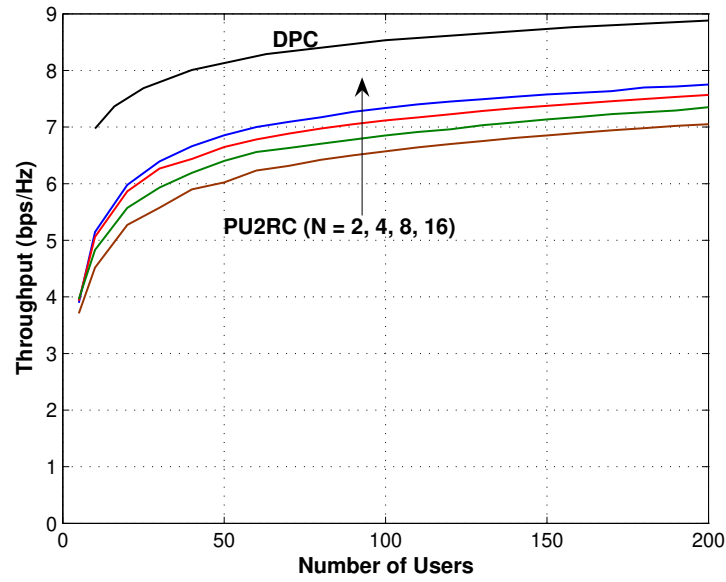


Fig. 7. Comparison between the throughput of PU2RC and its upper bound achieved by dirty paper coding (DPC) and multiuser iterative water-filling for an increasing number of users U , $\text{SNR} = 5$ dB, and the number of transmit antennas $N_t = 2$.

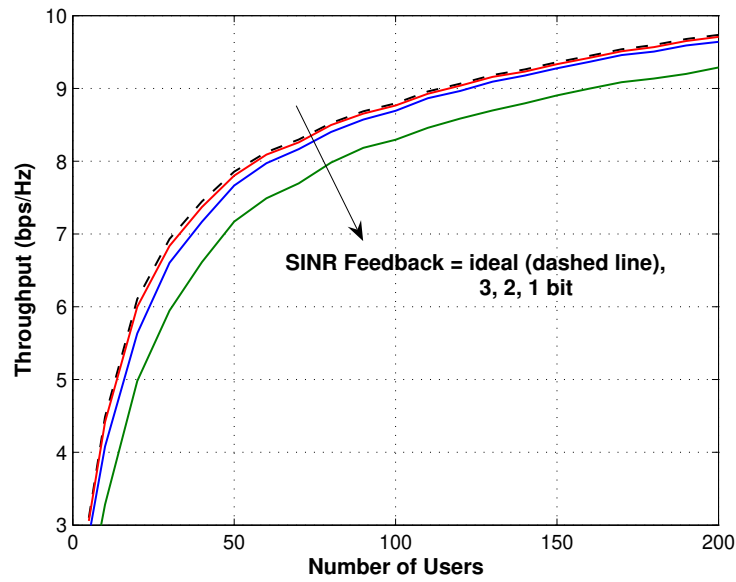


Fig. 8. The effect of SINR quantization for $\text{SNR} = 5$ dB, the number of transmit antennas $N_t = 4$, and the codebook size for channel shape quantization is $N = 16$.